Rhenium variations in molybdenite (MoS₂): Evidence for progressive subsurface oxidation

Joshua Golden [a], Melissa McMillan [a], Robert T. Downs [a], Grethe Hystad [b], Ian Goldstein [b], Holly J. Stein [c,d], Aaron Zimmerman [c], Dimitri A. Sverjensky [e,f], John T. Armstrong [f], Robert M. Hazen [f,*]

[a] Department of Geosciences, University of Arizona, 1040 East 4th Street, Tucson, AZ 85721, USA
[b] Department of Mathematics, University of Arizona, Tucson, AZ 85721-0089, USA
[c] AIRIE Program, Department of Geosciences, Colorado State University, Fort Collins, CO 80523-1482, USA
[d] Geological Survey of Norway, 7491 Trondheim, Norway
[e] Department of Earth and Planetary Sciences, Johns Hopkins University, Baltimore, MD 21218, USA
[f] Geophysical Laboratory, Carnegie Institution of Washington, 5251 Broad Branch Road, NW, Washington, DC 20015, USA

ARTICLE INFO

ABSTRACT

Temporal trends in Earth's near-surface mineralogy correlate with major events in Earth's geochemical and tectonic history. New and published analyses of 422 molybdenite (MoS₂) specimens from 135 localities with known ages from 2.91 billion years (Ga) to 6.3 million years (Ma) reveal two statistically significant trends. First, systematic increases in average and maximum trace concentrations of Re in molybdenite since 3.0 Ga point to enhanced oxidative weathering by subsurface fluids. In addition, episodic molybdenum mineralization correlates with five intervals of supercontinent assembly from ~2.7 Ga (Kenorland) to 300 Ma (Pangaea).

1. Introduction

Atmospheric oxygen has increased episodically over the past 2.5 billion years of Earth history. The protracted "Great Oxidation Event" (GOE) saw an increase from less than 0.001% to possibly greater than 1% of present atmospheric levels (PAL) during the Paleoproterozoic Era (~2.5–2.0 Ga), with additional increase to perhaps 10% of PAL following episodes of Neoproterozoic Era glaciation (Karhu and Holland, 1996; Farquhar et al., 2000; Canfield et al., 2000; Kump et al., 2001; Kasting, 2001; Holland, 2002; Hannah et al., 2004; Kump, 2008; Lyons et al., 2012).

An as yet unresolved question regards the rate and extent of widespread terrestrial subsurface oxygenation, which may have postdated the atmospheric GOE. Recent observations of transition element distributions through Earth history (Anbar et al., 2007; Scott et al., 2008; Konhauser et al., 2011; Planavsky et al., 2011; Hazen et al., 2012), coupled with calculations of near-surface redox conditions (Hazen et al., 2008, 2009; Sverjensky and Lee, 2010), suggest that a protracted interval of near-surface (< 2 km) oxidation

dramatically expanded the range of redox conditions into the stability fields of many previously unstable minerals, notably those of such transition elements as Fe, Ni, Co, Mn, Cu, Mo, and U. Accordingly, Hazen et al. (2008) estimated that approximately two-thirds of all known mineral species first appeared following the GOE as a result of near-surface oxidation.

The extent and timing of this protracted subsurface terrestrial oxidation interval can be documented through studies in mineral evolution, which explore temporal changes in Earth's near-surface mineralogy, including diversity of species; relative abundances of species; and compositional ranges of major, minor, and trace elements (Grew and Hazen, 2009, 2010; Hazen et al., 2011, 2012; Hazen and Papineau, 2012). In this contribution we summarize data on Re as a trace element in molybdenite, which represents a possible mineralogical proxy for shallow (< 2 km) subsurface oxidation (e.g., White et al., 1981). We chose molybdenite to probe the extent and timing of subsurface oxidation for 4 principal reasons. First, molybdenite is a relatively common mineral, usually of magmatic-hydrothermal origins (White et al., 1981; Stein et al., 2003; Stein, 2006; Audétat, 2010), with more than 4000 reported localities (http://mindat.org) spanning more than 3 Ga. Second, molybdenite commonly incorporates Re and other redox-sensitive transition elements as trace constituents

* Corresponding author. Tel.: +1 202 478 8962; fax: +1 202 478 8901.
E-mail address: rhazen@ciw.edu (R.M. Hazen).

and thus is likely to reflect changing geochemical environments through time; both Mo and Re are insoluble in their more reduced tetravalent forms, whereas Mo^{6+} and Re^{7+} are more soluble in aqueous solutions and are thus mobilized under more oxidizing conditions (e.g., Crusius et al., 1996; Algeo and Lyons, 2006; Miller et al., 2011). Third, development of the Re–Os chronometer for molybdenite permits determination of accurate ages for specific molybdenite samples; the study of molybdenite thus avoids some of the pitfalls associated with dating minerals whose ages depend on the analysis of coexisting phases that may not be contemporaneous (Stein et al., 2001). And fourth, the element Mo exemplifies mineral co-evolution with biology, for example in its role in the nitrogen fixation enzyme nitrogenase (Schwartz et al., 2009; Zehr and Ward, 2002; Rees et al., 2005). Variations of Mo mineral distribution through Earth history may thus shed light on the biological Mo cycle.

2. Results and discussion

Our results are based on Re analyses of 422 molybdenite samples from 135 localities of known ages (Supporting Materials: Table 1 and KML GoogleMaps file). We measured molybdenite trace element concentrations in 24 samples, using inductively coupled plasma mass spectrometry, scanning electron microscopy, and electron microprobe analyses. We detected significant amounts of Fe, W, and Re (to ∼1000, 4000, and 5000 ppm, respectively), as well as elevated (>20 ppm, but <1000 ppm) Ni, Mn, Cu, Ru, Ca, and/or Co in several samples. We supplemented these data with Re data in 398 additional molybdenite samples described in the diverse published mineralogical and economic geology literature.

These data must be viewed with two important caveats. First, in some published studies that employ Re–Os dating techniques the Re content (in ppm) may be reported for a sample in which fine-grained disseminated molybdenite is mixed with other phases—a situation not generally documented in these publications. Thus, the Re content of the pure molybdenite in some specimens may be significantly greater than (but not less than) the values reported in Supplementary Table 1. A second uncertainty relates to the possibility of multiple age components in individual molybdenite grains, as documented by Aleinkoff et al. (2012) for Proterozoic specimens from the Hudson Highlands, New York. However, the total age range determined in their study (∼941–954 Ma) is narrow compared to the broad temporal features considered here.

2.1. Molybdenite and subsurface oxidation

We observe significant trends in average and maximum Re trace element concentration in molybdenite versus time (Fig. 1; Tables 1 and 2). In Table 1 we report the average and maximum Re values for 6 equal sized bins of molybdenite samples arranged chronologically. Thus, the oldest 71 samples in our compilation, which range in age from 2.91 to 1.87 Ga, have an average Re value of 115 ppm and a maximum value of 832 ppm. This bin contrasts with the most recent 70 molybdenite samples, all deposited in the last 62 Ma, which have an average Re content of 453 ppm and a maximum of 10,424 ppm.

Table 2 records average Re concentrations in molybdenites from six major geological time periods. The average Re concentration of the 49 oldest specimens of Archean age (≥ 2.5 Ga) in our study is 71.0 ppm, with a maximum observed 832 ppm Re from the Boddington gold mine, Australia (see Supplementary Table). Paleoproterozoic Era data (2.5–1.6 Ga) are sparse, with only 35 specimens from 4 localities that average 134 ppm Re (maximum 623 ppm). During the Mesoproterozoic and Neoproterozoic Eras
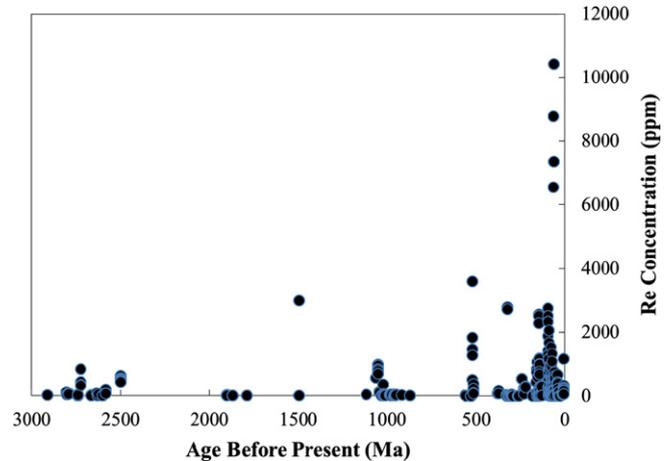

Fig. 1. Rhenium content (ppm) is plotted versus age (Ga) for 422 molybdenite specimens from 135 localities. The average Re concentration for 49 specimens of Archean age (> 2.5 Ga) is 71 ppm, with a maximum value of 832 ppm Re (see Table 1). Since 2.5 Ga, values increase systematically, reaching an average of 589 ppm and a maximum value of 10,424 ppm for 82 specimens formed during the Cenozoic Era (< 65.5 Ma).

Table 1
Age intervals, number of specimens, average values of Re content, and maximum recorded values for Re content in 422 molybdenite samples arranged chronologically into bins of equal size (see Supplementary Table 1).

Age interval (Ga)	♯ Specimens	Average Re (ppm)	Maximum Re (ppm)
2.91–1.87	71	115	832
1.87–0.528	71	144	2992
0.528–0.155	70	335	2772
0.154–0.092	70	508	2740
0.092–0.062	70	555	8785
0.062–0.006	70	453	10424

Table 2
Age intervals, number of specimens, average values of Re content, and maximum recorded values for Re content in 422 molybdenite samples divided into bins according to major geological time intervals (see Supplementary Table 1).

Age interval (Ma)	♯ Specimens	Average Re (ppm)	Maximum Re (ppm)
Archean Eon (> 2500)	49	71	832
Paleoproterozoic Era (2500–1600)	35	134	623
Meso/Neoproterozoic Eras (1600–542)	55	185	2992
Paleozoic Era (542–251)	46	339	3606
Mesozoic Era (251–65.5)	155	425	2740
Cenozoic Era (< 65.5)	82	589	10424

(1.6–0.542 Ga) the average Re concentration of 55 specimens is 185 ppm with a maximum of 2992 ppm in a specimen from the Kabeliai prospect in Lithuania. The average for 46 Paleozoic Era samples (542–251 Ma) is 339 ppm with a maximum value of 3606 ppm in a molybdenite specimen from Otjozonjati, Namibia. The 155 Mesozoic Era (251–65.5 Ma) specimens in our survey have an average Re content of 425 ppm and a maximum value of 2740 ppm in a sample from the Elatsite Mine, Bulgaria. The most recent 82 samples from the Cenozoic Era (< 65.5 Ma) have the highest average value, 589 ppm, as well as the highest individual Re content of any recorded sample—10,424 ppm in a specimen from El Alacrán, Mexico.

These data reveal a significant systematic increase in the average and maximum Re content of molybdenite from the Archean Eon (>2.5 Ga) through the Phanerozoic Eon (<542 Ma). To test the significance of Re content as a function of time, we conducted a linear regression analysis of the log of the Re content as a function of time, using indicator variables as described in Montgomery et al. (2006). In this method the regression equation is:

$$\log(\text{Re}) = \beta_0 + \beta_1 t + \beta_2 x_2 + \beta_3 x_3 + \beta_4 x_4 + \beta_5 x_5 + \beta_6 x_6,$$

where t is time and β_i are regression parameters, and x_i are indicators variables. Indicator variables are set to 0 or 1 depending on which era the data point is in. For example, in this analysis, x_6 represents the newest era, the Cenozoic, and a data point from this era has $x_6 = 1$ while $x_2 = x_3 = x_4 = x_5 = 0$. This analysis provided the refined parameters, as follows: $\beta_0 = -14(2)$, $\beta_1 = 0.0059(8)$, $\beta_2 = 4.6(7)$, $\beta_3 = 12(2)$, $\beta_4 = 15(2)$, $\beta_5 = 18(2)$, and $\beta_6 = 19(2)$. In particular, the value for β_1 indicates a significant increase in average log(Re) concentration with respect to time, with a slope 7 times greater than its standard deviation. In addition, the other parameters indicate that the partitioning of data into the various eras is statistically significant.

While the data are too few and too episodic (see below) to document whether these changes in Re content are gradual or punctuated, the overall increase through time is evident (Tables 1 and 2; Fig. 1). At least two alternative explanations for this trend should be considered. On the one hand, it is well established that the character of major ore deposits has changed considerably through Earth history as a consequence of changing modes of intrusion and compositions of associated fluids (e.g., Meyer, 1981). Accordingly, increases in the Re content of molybdenite might, in part, reflect systematic variations in the temperature, depth, magmatic composition, or host lithology of the mineralized zone. However, given the strong influence of redox conditions on the mobilization of Re, we suggest that the observed trends in Re content of molybdenite primarily reflect increasing near-surface oxidation following the GOE and Neoproterozoic glaciations. Extensive subsurface oxidative weathering may be required to mobilize significant quantities of Re (average concentration 0.5 ppb in the crust) compared to Mo. Our data, in concert with analyses of Mo concentrations in black shale (Scott et al., 2008), suggest that the near-surface geochemical cycles of Re and Mo may have been increasingly coupled during the last 2.5 Ga. This interpretation is consistent with conclusions reached in studies of other redox-sensitive elements (Meyer, 1981; Nash et al., 1981; Anbar et al., 2007; Hazen et al., 2009; Konhauser et al., 2011; Kump et al., 2011).

Our data do not yet incorporate information on depth of molybdenite formation, which might be gleaned from mineralogical geobarometers, as well as lithologies and textures of host igneous rocks. A plausible hypothesis is that deeper crustal zones on average took longer to experience the influence of atmospheric oxidation through the circulation of oxygenated ground waters. Thus, a systematic trace element survey that also incorporates depth information might point to stages in subsurface oxidation, which in turn might hold the key to the timing of Earth's post-GOE mineralogical diversification.

2.2. Molybdenite and the supercontinent cycle

Data on ages of molybdenite samples reveal episodicity, with statistically significant pulses of mineralization at 2.85–2.60 Ga, 1.95–1.85 Ga, 1.10–0.90 Ga, 0.60–0.50 Ga, and 0.4–0.2 Ga—all intervals that approximately correlate with periods of supercontinent assembly (e.g., Condie et al., 2009; Santosh et al., 2009; Bradley, 2011; Hazen et al., 2012; Fig. 2). Though data are few prior to the Neoproterozoic Era (1.0–0.542 Ga), we applied standard peak-fitting protocols to the age versus locality data in the Supplementary Table.
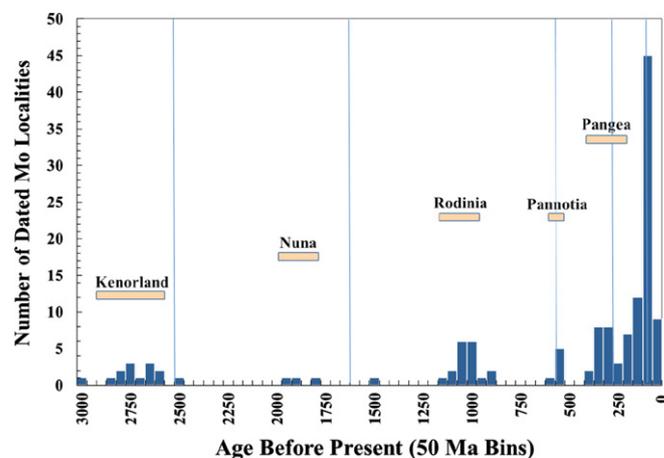

Fig. 2. Histogram of age versus number of mineralized districts for molybdenite samples from 135 localities dated using Re–Os methods. These data fit to 5 statistically significant Gaussian curves with maxima at 2704 ± 24, 998 ± 13, 548 ± 17, 304 ± 7, and 84 ± 5 Ma. Note the correlation of the first four of these maxima with intervals of supercontinent assembly—a pattern also observed in the ages of zircon grains (Campbell and Allen, 2008; Hawkesworth et al., 2010; Condie and Aster, 2010) and in the ages of Hg, Be, and B mineralization (Grew and Hazen, 2009, 2010; Hazen et al., 2012). Only 4 localities have ages between 2.50 and 1.12 Ga, and 3 of those ages fall in the period when the supercontinent Nuna is thought to have assembled ($\sim$2.0–1.8 Ga).

(Note that while there is no theoretical justification for employing any particular peak shape, we employed Gaussian peak fitting procedures for convenience.) The data fit to four statistically significant Gaussian curves with maxima at 2704 ± 24, 998 ± 13, 548 ± 17, and 304 ± 7 Ma. Additionally, 3 localities cluster in ages between 1.90 and 1.79 Ga, but are insufficient to define a peak. These 5 periods of maximum molybdenite mineralization are separated by temporal gaps at 2.50 – 1.90 Ga (no recorded localities), 1.78 – 1.06 Ga (2 recorded localities), 870 – 570 Ma (no recorded localities), and 510 – 380 Ma (no recorded localities).

The ages of maximum molybdenite mineralization correlate with estimated times of assembly of the supercontinents of Kenorland (also referred to as Superia), Rodinia, Pannotia (including Gondwana), and Pangaea (Condie, 1989; Barley et al., 2005; Rogers and Santosh, 2009; Bogdanova et al., 2009; Condie et al., 2009; Santosh et al., 2009). In addition, three molybdenite localities occur during the presumed interval of Nuna assembly (also referred to as Columbia) at $\sim$2.0–1.8 Ga, whereas only a single locality is recorded for the subsequent 500 million years of Nuna stability and breakup. We also document an as yet unexplained maximum in the frequency of molybdenite mineralization during the interval between 55 and 95 million years ago (Fig. 2). This feature may, in part, reflect a preservational bias toward more recent deposits, but significant differences among B, Be, U, Hg, and Mo mineralization patterns during the last 100 million years suggest that other as yet unidentified factors may play key roles in this late-Mesozoic and early Cenozoic molybdenite pulse (Nash et al., 1981; Hazen et al., 2009, 2012; Grew et al., 2011).

More than 3 billion years of mineralogical episodicity has been observed for zircon grains (Campbell and Allen, 2008; Hawkesworth et al., 2010; Condie and Aster, 2010; Condie et al., 2011); for minerals of beryllium (Grew and Hazen, 2009), boron (Grew and Hazen, 2010), and mercury (Hazen et al., 2012); as well as for the formation of complex pegmatites (Tkachev, 2011). These significant mineralization events correlate with continental collisions and igneous activity associated with orogenies at convergent margins. The episodic pulses of Mo mineralization dating back to almost 3 Ga suggest that even though Mo is a trace element in Earth's crust (average concentration 1 ppm) it was

cycled repeatedly through geologic processes since the beginning of modern plate tectonics ≥ 3.0 Ga ago (Shirey and Richardson, 2011; Van Kranendonk, 2011).

3. Conclusions

Earth's rich record of molybdenite mineralization reveals two important trends that reflect global geochemical and tectonic evolution. First, the incorporation of Re and other redox-sensitive trace elements changes dramatically through Earth history, with average Re content in molybdenite increasing by a factor of 8 over the past 3 billion years. This increase may reflect the enhanced mobility of Re in a subsurface environment gradually exposed to a more oxidized aqueous environment. Subsurface oxidation was thus an important consequence of the atmospheric GOE, albeit one whose influence on subsurface mineralogy may have been delayed by hundreds of millions of years.

Secondly, the temporal distribution of molybdenite samples amplifies the growing body of data that points to the highly episodic nature of crustal mineralization through the past 3 billion years of Earth history. Mineralization increased dramatically during episodes of continental convergence and supercontinent assembly, whereas intervals of supercontinent stability and breakup were characterized by a dearth of molybdenite and other metal deposits.

Finally, it would be of great interest to integrate the study of these and other dated molybdenite samples with other systematic investigations. For example, correlations of locality and age information with detailed information on host lithologies and paleotectonic settings of these molybdenite localities might provide insights on changing patterns of mineralization in deep time. In addition, a number of geochemical and biological processes have the potential to fractionate the 7 stable isotopes of molybdenum (Anbar, 2004; Hannah et al., 2007), and thus such data, especially in concert with trace and minor element compositions, have the potential to shed new light on Earth history.

Appendix A. Supplementary material

Supplementary data associated with this article can be found in the online version at http://dx.doi.org/10.1016/j.epsl.2013.01.034. These data include Google map of the most important areas described in this article.

References

Aleinkoff, J.N., Creaser, R.A., Lowers, H.A., Magee Jr., C.W., Grauch, R.I., 2012. Multiple age components in individual molybdenite grains. Chem. Geol. 300–301, 55–60.

Algeo, T.J., Lyons, T.W., 2006. Mo-total organic carbon covariation in modern anoxic marine environments: implications for analysis of paleoredox and paleohydrographic conditions. Paleoceanography 21, http://dx.doi.org/10.1029/2004PA001112.

Anbar, A.D., 2004. Molybdenum stable isotopes: observations, interpretations and directions. Rev. Mineral. Geochem. 55, 429–454.

Anbar, A.D., Duan, Y., Lyons, T.W., Arnold, G.L., Kendall, B., Creaser, R.A., Kaufman, A.J., Gordon, G.W., Scott, C., Garvin, J., Buick, R., 2007. A whiff of oxygen before the Great Oxidation Event. Science 317, 1903–1906.

Audétat, A., 2010. Source and evolution of molybdenum in the porphyry Mo(-Nb) deposit at Cave Peak, Texas. J. Petrol. 51, 1739–1760.

Barley, M.E., Bekker, A., Krapez, B., 2005. Late Archean to Early Proterozoic global tectonics, environmental change and the rise of atmospheric oxygen. Earth Planet. Sci. Lett. 238, 156–171.

Bogdanova, S.V., Pisarevsky, S.A., Li, Z.X., 2009. Assembly and breakup of Rodinia (some results of IGCP Project 440). Stratigr. Geol. Correlation 17, 259–274.

Bradley, D.C., 2011. Secular trends in the geologic record and the supercontinent cycle. Earth-Sci. Rev. 108, 16–33.

Campbell, I.H., Allen, C.M., 2008. Formation of supercontinents linked to increases in atmospheric oxygen. Nat. Geosci. 1, 554–558.

Canfield, D.E., Habicht, K.S., Thamdrup, B., 2000. The Archean sulfur cycle and the early history of atmospheric oxygen. Science 288, 658–661.

Condie, K.C., 1989. Plate Tectonics and Crustal Evolution, 3rd edition Pergamon Press.

Condie, K.C., Aster, R.C., 2010. Episodic zircon age spectra of orogenic granitoids: the supercontinent connection and continental growth. Precambrian Res. 180, 227–236.

Condie, K.C., Belousova, E., Griffin, W.L., Sircombe, K.N., 2009. Granitoid events in space and time: constraints from igneous and detrital zircon age spectra. Gondwana Res. 15, 228–242.

Condie, K.C., Bickford, M.E., Aster, R.C., Belousova, E., Scholl, D.W., 2011. Episodic zircon ages, Hf isotopic composition, and the preservation rate of continental crust. GSA Bull. 123, 951–957.

Crusius, J., Calvert, S., Pederson, T., Sage, D., 1996. Rhenium and molybdenum enrichments in sediments as indicators of oxic, suboxic and sulfidic conditions of deposition. Earth Planet. Sci. Lett. 145, 65–78.

Farquhar, J., Bao, H., Thiemans, M.H., 2000. Atmospheric influence of Earth's earliest sulfur cycle. Science 289, 756–758.

Grew, E.S., Hazen, R.M., 2009. Evolution of the minerals of beryllium, a quintessential crustal element. Geological Society of America Abstracts with Program 41, 99.

Grew, E.S., Hazen, R.M., 2010. Evolution of boron minerals: has early species diversity been lost from the geological record? Geological Society of America Abstracts with Program, 42, 92.

Grew, E.S., Bada, J.L., Hazen, R.M., 2011. Borate minerals and origin of the RNA world. Orig. Life Evol. Biosph. 41, 307–316, http://dx.doi.org/10.1007/s11084-101-9233-y.

Hannah, J.L., Bekker, A., Stein, H.J., Markey, R.J., Holland, H.D., 2004. Primitive Os and 2316 Ma age for marine shale: implications for Paleoproterozoic glacial events and the rise of atmospheric oxygen. Earth Planet. Sci. Lett. 225, 43–52.

Hannah, J.L., Stein, H.J., Wieser, M.E., de Laeter, J.R., Varner, M., 2007. Mo isotope variations in molybdenite: vapor transport and Rayleigh fractionation of Mo. Geology 35, 703–706.

Hawkesworth, C.J., Dhuime, B., Pietranik, A.B., Kemp, A.I.S., Storey, C.D., 2010. The generation and evolution of continental crust. J. Geol. Soc. 167, 229–248.

Hazen, R.M., Papineau, D., 2012. Mineralogical co-evolution of the geosphere and biosphere. In: Knoll, A.H., Canfield, D.E., Konhauser, K.O. (Eds.), Fundamentals of Geobiology. Wiley-Blackwell, Oxford UK, pp. 333–350.

Hazen, R.M., Papineau, D., Bleeker, W., Downs, R.T., Ferry, J.M., McCoy, T.J., Sverjensky, D.A., Yang, H., 2008. Mineral evolution. Am. Mineral. 93, 1693–1720.

Hazen, R.M., Ewing, R.C., Sverjensky, D.A., 2009. Evolution of uranium and thorium minerals. Am. Mineral. 94, 1293–1311.

Hazen, R.M., Bekker, A., Bish, D.L., Bleeker, W., Downs, R.T., Farquhar, J., Ferry, J.M., Grew, E.S., Knoll, A.H., Papineau, D.F., Ralph, J.P., Sverjensky, D.A., Valley, J.W., 2011. Needs and opportunities in mineral evolution research. Am. Mineral. 96, 953–963.

Hazen, R.M., Golden, J., Downs, R.T., Hystad, G., Grew, E.S., Azzolini, D., Sverjensky, D.A., 2012. Mercury (Hg) mineral evolution: a mineralogical record of supercontinent assembly, changing ocean geochemistry, and the emerging terrestrial biosphere. Am. Mineral. 97, 1013–1042.

Holland, H.D., 2002. Volcanic gases, black smokers, and the great oxidation event. Geochim. Cosmochim. Acta 66, 3811–3826.

Karhu, J.A., Holland, H.D., 1996. Carbon isotopes and the rise of atmospheric oxygen. Geology 24, 867–870.

Kasting, J., 2001. The rise of atmospheric oxygen. Science 293, 819–820.

Konhauser, K.O., Lalonde, L.V., Planavsky, N.J., Pecoits, E., Lyons, T.W., Mojzsis, S.J., Rouxel, O.J., Barley, M.E., Rosiere, C., Fralick, P.W., Kump, L.R., Bekker, A., 2011. Aerobic bacterial pyrite oxidation and acid rock drainage during the Great Oxidation Event. Nature 478, 369–373.

Kump, L.R., 2008. The rise of atmospheric oxygen. Nature 451, 277–278.

Kump, L.R., Kasting, J.F., Barley, M.E., 2001. Rise of atmospheric oxygen and the "upside down" Archean mantle. Geochem. Geophys. Geosyst. 2 2000GC000114.

Kump, L.R., Junium, C., Arthur, M.A., Brasier, A., Fallick, A., Melezhik, V., Lepland, A., črne, A., Luo, G., 2011. Isotopic evidence for massive oxidation of organic matter following the Great Oxidation Event. Science 334, 1694–1696.

Lyons, T.W., Reinhard, C.T., Love, G.D., Xiao, S., 2012. Geobiology of the Preterozoic Eon. In: Knoll, A.H., Canfield, D.E., Konhauser, K.O. (Eds.), Fundamentals of Geobiology. Wiley-Blackwell, Oxford UK, pp. 371–402.

Meyer, C., 1981. Ore-forming processes in geologic history. Economic Geology 75th Anniversary Volume, pp. 6–41.

Miller, C.A., Peucker-Ehrenbrink, B., Walker, B.D., Marcantonio, F., 2011. Re-assessing the surface cycling of molybdenum and rhenium. Geochim. Cosmochim. Acta 75, 7146–7179.

Montgomery, D.C., Peck, E.A., Vining, G.G., 2006. Introduction to Linear Regression Analysis, fourth edition John Wiley & Sons, Hoboken, New Jersey, pp. 612.

Nash, J.T., Granger, H.C., Adams, S.S., 1981. Geology and concepts of genesis of important types of uranium deposits. Economic Geology 75th Anniversary Volume, pp. 63–116.

Planavsky, N.J., McGoldrick, P., Scott, C.T., Li, C., Reinhard, C.T., Kelly, A.E., Chu, X., Bekker, A., Love, G.D., Lyons, T.W., 2011. Widespread iron-rich conditions in the mid-Proterozoic ocean. Nature 477, 448–451.

Rees, D.C., Tezcan, F.A., Haynes, C.A., Walton, M.Y., Andrade, S., Einsle, O., Howard, J.B., 2005. Structural basis of nitrogen fixation. Philos. Trans. R. Soc. London A363, 971–984.

Rogers, J.J.W., Santosh, M., 2009. Tectonics and surface effects of the super-continent Columbia. Gondwana Res. 15, 373–380.

Santosh, M., Maruyama, S., Yamamoto, S., 2009. The making and breaking of supercontinents: some speculations based on superplumes, super downwelling and the role of tectosphere. Gondwana Res. 15, 324–341.

Schwartz, G., Mendel, R.R., Ribbe, M.W., 2009. Molybdenum cofactors, enzymes and pathways. Nature 460, 839–847.

Scott, C., Lyons, T.W., Bekker, A., Shen, Y., Poulton, S.W., Anbar, A.D., 2008. Tracing the stepwise oxygenation of the Proterozoic ocean. Nature 452, 456–459.

Shirey, S.B., Richardson, S.H., 2011. Start of the Wilson Cycle at 3 Ga shown by diamonds from the subcontinental mantle. Science 333, 434–436, http://dx.doi.org/10.1126/science.1206275.

Stein, H.J., 2006. Low-rhenium molybdenite by metamorphism in northern Sweden: recognition, genesis, and global implications. Lithos 87, 300–327.

Stein, H.J., Markey, R.J., Morgan, J.W., Hannah, J.L., Scherstén, A., 2001. The remarkable Re–Os chronometer in molybdenite: how and why it works. Terra Nova 13, 479–486.

Stein, H., Scherstén, A., Hannah, J., Markey, R., 2003. Sub-grain scale decoupling of Re and ^{187}Os and assessment of laser ablation ICP-MS spot dating in molybdenite. Geochim. Cosmochim. Acta 67, 3673–3686.

Sverjensky, D.A., Lee, N., 2010. The Great Oxidation Event and mineral diversification. Elements 6, 31–36.

Tkachev, A.V., 2011. Evolution of metallogeny of granitic pegmatites associated with orogens throughout geological time. Geol. Soc. London Spec. Publ. 350, 7–23, http://dx.doi.org/10.1144/SP350.2 0305-8719.

Van Kranendonk, M.J., 2011. Onset of plate tectonics. Science 333, 413–414.

White, W.H., Bookstrom, A.A., Kamilli, R.J., Ganster, M.W., Smith, R.P., Ranta, D.E., Steininger, R.C., 1981. Character and origin of Climax-type molybdenum deposits. Economic Geology 75th Anniversary Volume, pp. 270–316.

Zehr, J.P., Ward, B.B., 2002. Nitrogen cycling in the ocean: new perspectives on processes and paradigms. Appl. Environ. Microbiol. 68, 1015–1024.